Journal of Photochemistry and Photobiology A: Chemistry 337 (2017) 132–139

Contents lists available at ScienceDirect

Journal of Photochemistry and Photobiology A: Chemistry

journal homepage: www.elsevier.com/locate/jphotochem

Photocatalytic inactivation of highly resistant microorganisms in water: A kinetic approach

Luz Luz del Carmen Huesca-Espitia[a], Veronica Aurioles-López[a], Irwing Ramírez[a], Jose Luis Sánchez-Salas[a], Erick R. Bandala[b,*]

[a] Universidad de Las Américas, Puebla. Sta. Catarina Martir, Cholula 72810, Puebla, Mexico
[b] Division of Hydrologic Sciences, Desert Research Institute (DRI), 755 E, Flamingo Road, Las Vegas 89119-7363, NV, USA

ARTICLE INFO

Article history:
Received 25 February 2016
Received in revised form 26 September 2016
Accepted 20 January 2017
Available online 23 January 2017

Keywords:
Inactivation
Bacillus subtilis spores
Advanced oxidation processes
Photoassisted Fenton reaction
Mechanisms

ABSTRACT

The mechanism for the photocatalytic inactivation of highly resistant microorganisms (i.e., *Bacillus subtilis* spores) in water was studied using a kinetic approach. This required characterizing the basic processes that occur within the photoreactor. The radiative intensity that entered the photocatalytic system was estimated using the ferrioxalate actinometrical process, the amount of hydroxyl radical produced under a specific photo-assisted Fenton reaction was measured, and a kinetic model to predict the hydroxyl radical generation was proposed to fit the experimental values. These results were then used to suggest new assessment related to the spore inactivation mechanism under controlled photo Fenton reaction conditions. The kinetic model was found to fit the experimental data fairly well ($r^2 > 0.99$) and hydroxyl radical generation was determined to significantly affect the inactivation process. It was determined that a specific amount of hydroxyl radical is required to overwhelm the self-repairing mechanisms of the cell and cause cell death. The amount of hydroxyl radicals generated was found to be a function of radiative intensity and reagent concentration, as previously reported. The proposed relationship between the amount of hydroxyl radical and the inactivation process was supported by adding chloride ions to acting as radical scavengers. It was observed that even the lowest chloride ion concentration was capable of producing a significant delay in the inactivation process by scavenging hydroxyl radicals and generating low reactive species at the pH conditions tested.

1. Introduction

The spread of waterborne diseases resulting from a lack of access to safe drinking water is a critical global concern. It is estimated that over 1.2 billion people around the world do not have access to drinking water supply services, usually because of poverty [1]. The effects of waterborne diseases on sustainable economic development in developing countries and some areas of developed countries are expected to increase because climate-change-related temperature anomalies, which can alter the concentration, persistence, growth rate, and survival of many pathogens in water [2]. Reduced precipitation, changes in rain patterns and the projected rise in seasonal and annual air temperatures are to affect the survival of existing and emerging pathogens and increase the incidence of microbial diseases [3,4]. It has been estimated that there will be increasing impacts to public health because of increased incidences of existing waterborne diseases and the emergence of unknown diseases [5].

Advanced oxidation processes (AOPs) have proven to be a promising alternative to inactivate pathogens in water. AOPs have been tested for their ability to inactivate several different pathogens [6,7]. In particular, Fenton and Fenton-like processes have been identified as effective alternatives for inactivating highly resistant microorganisms [8–10]. *Bacillus subtilis* spores are highly resistant to a wide variety of stressing conditions—such as toxic chemicals, high pressure and temperature, UV, and ionizing radiation—which make them useful test microorganisms for photocatalytic disinfection processes [11] and a conservative water-disinfection model [9,12]. Although current literature has reported successful inactivation of *B. subtilis* spores using Fenton-like AOPs, little is known about the inactivation process. Understanding the mechanisms of the inactivation process will provide the required knowledge to analyze, design, and improve full-scale applications that can be used to implement adaptation measures to prevent the projected effects of climate change on microbiological water quality and the associated effects on public

* Corresponding author.
E-mail address: erick.bandala@dri.edu (E.R. Bandala).

http://dx.doi.org/10.1016/j.jphotochem.2017.01.025
1010-6030/

health. The goal of this work is to determine the mechanisms for inactivating *B. subtilis* spores in water using Fenton-like AOPs.

2. Experimental procedures

2.1. Reagents

The reagents used in this work were sodium chloride (NaCl, Merck), sulfuric acid (H_2SO_4, Sigma), sodium hydroxide (NaOH, Sigma), *N*,*N*-dimethyl-*p*-nitrosoaniline (pNDA, Sigma), potassium dichromate ($K_2Cr_2O_7$, Aldrich), diphenylamine, 1,10-phenanthroline (Sigma), ferrous sulfate ($FeSO_4$, Sigma), and hydrogen peroxide (H_2O_2, 50% stabilized, Sigma). All reagents were purchased as reagent grade (A.C.S.) and used as received without further purification.

2.2. Experimental setup

Inactivation tests were performed in the experimental setup shown in Fig. 1. Two low-pressure UV lamps (λ_{max} = 365 nm, 15 W, GE F1578/BLB) with an OF-365AUV (black) Filter from Spectroline® (cutting wavelength 365 nm) were used as a radiation source. The photoreactor used included a jacketed reservoir (500 mL) connected to a temperature controller (Polystat®, Cole Parmer) in order to get all the experimental runs at 20 ± 0.1 °C. A magnetic stirrer was used to keep the reaction mixture suspended.

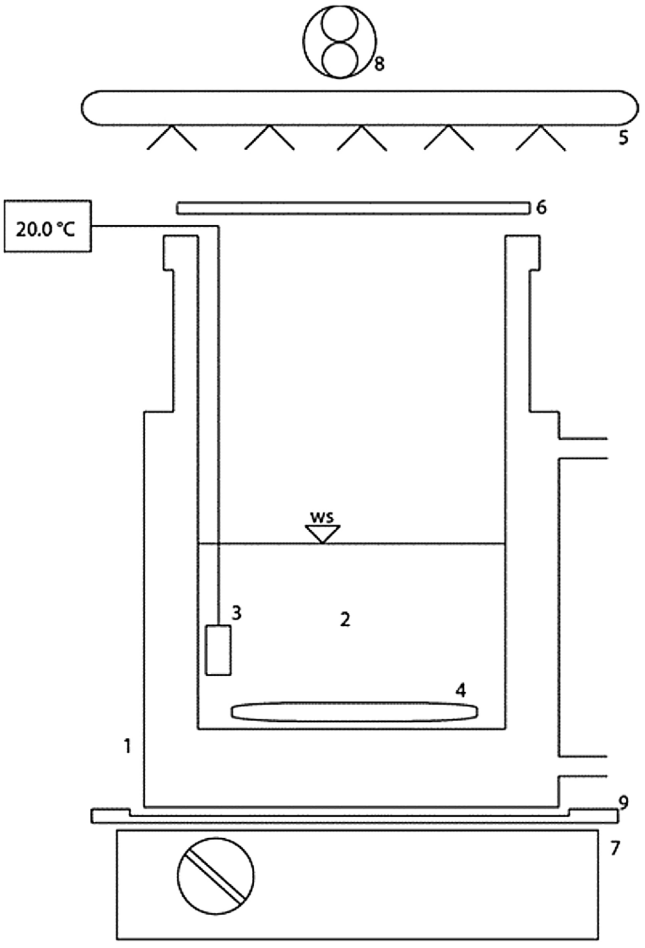

Fig. 1. Experimental setup used in this work. The main arrangement elements are: 1) jacketed photoreactor connected to a controlled temperature water bath, 2) reaction mixture, 3) temperature measurement, 4) magnetic stirrer, 5) BL lamps, 6) OF-365AUV (black) optical filter, 7) magnetic stirring plate, 8) air extraction system, and 9) horizontal positioner.

2.3. Actinometry measurements

The radiative intensity entering the photoreactor during the inactivation process was measured using the widely reported ferrioxalate actinometry procedure [13]. It is well-known that potassium ferrioxalate can absorb UV radiation in agreement with Eq. (1) as follows:

$$2Fe^{3+} + C_2O_4^{2-} \xrightarrow{h\nu} 2Fe^{2+} + 2CO_2 \quad (1)$$

The amount of ferrous ion produced can be quantified by complexation with 1,10-phenanthroline and measuring its absorbance at 510 nm [14].

The amount of radiation arriving into the system by unit of time (I) can be estimated in agreement with Eq. (2) as follows:

$$I = \frac{d[Fe^{2+}]V}{dt \quad \phi} \quad (2)$$

where I is the photonic flux (Einstein min^{-1}), [Fe^{2+}] is the amount of ferrous ion measured by complexation with 1,10-phenanthroline at 510 nm, V is the irradiated volume (L), and ϕ is the ferrous ion quantum yield (1.21 Fe^{2+} quantum^{-1} at 365 nm) [15].

The radiative intensity was determined at four distances (8, 10, 13, and 15 cm) from the lamps to determine the highest value and was used to perform the inactivation processes and hydroxyl radical production processes with a known radiative intensity.

2.4. Hydroxyl radical production

The amount of hydroxyl radicals generated by the system was estimated using *N*,*N*-dimethyl-*p*-nitrosoaniline (pNDA) as a radical scavenger (Bors et al., 1978; Barashkov et al., 2010). As has been shown in previous reports, pNDA reacts with hydroxyl radicals with a 1:1 stoichiometry and at a high reaction ratio (k = 1.25 × 10^{10} $M^{-1}s^{-1}$), which is shown in Eq. (3) as follows (Farhataziz, 1977; Bors et al., 1978; Barashkov et al., 2010):

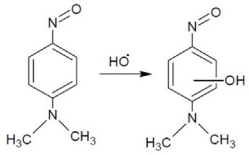

The determination of hydroxyl radical production was performed using 300 mL of pNDA (10 μM) and three different concentrations of ferrous ion (0.0, 0.018, and 0.036 mM) and hydrogen peroxide (0.0, 0.55, and 1.1 mM) for the Fenton-like process. Once the pNDA solution was poured in the photoreactor, the pH was adjusted to 3.0 with 0.1 M H_2SO_4, and then the required amount of ferrous sulfate was added and the mixture was stirred for 3 min to allow iron dissolution. After iron dissolution, the initial (t = 0) sample was taken (c.a. 1 mL). Finally, the required amount of hydrogen peroxide to get the desired final concentration was added to the reaction mixture and submitted under the lamps (previously warmed up for 15 min). The photocatalytic process was considered to have started once the hydrogen peroxide was added and the lamps were turned on. Further sampling was performed at 5, 10, 15, 25, 35, 45, and 60 min and the remaining concentration of pNDA was measured by absorption at 440 nm in a UV–vis spectrophotometer (Cary 100, Agilent).

2.5. Hydroxyl radical production kinetic model

The amount of hydroxyl radicals being produced for the specific reaction conditions described in Section 2.4 can be estimated by measuring the photocatalytic discoloration of pNDA and using the reaction stoichiometry shown in Eq. (3). Slightly discoloration of pNDA was found to occur even when Fenton reagents were not added into the photoreactor, so pNDA photolysis must also be considered to properly estimate hydroxyl radical generation. The overall pNDA discoloration process that resulted from AOP hydroxyl radical generation can be estimated using Eq. (4) as follows:

$$pNDA \overset{k_0,k_1}{\rightarrow} pNDA^* \tag{4}$$

where pNDA is the chemical species that shows the radiation absorption at 440 nm, pNDA* is the species generated after radical scavenging that does not absorb at 440 nm, k_0 is the photolysis reaction rate constant, and k_1 is the photocatalytic reaction rate constant. The overall discoloration process because of OH radical scavenging by pNDA can be described by Eq. (5) as follows:

$$\frac{d[pNDA]}{dt} = -k_0 - k_1[pNDA] \tag{5}$$

where [pNDA] is the concentration of pNDA and t is the reaction time. Eq. (5) can be solved by variable separation. After integration and normalization to the concentration of pNDA at time zero ($pNDA_0$), we obtain:

$$\frac{[pNDA]}{[pNDA]_0} = -\frac{k_0}{k_1} + \left[1 + \frac{k_0}{pNDA_0}\right] e^{-k_1 t} \tag{6}$$

The numerical solution of Eq. (6) can be obtained by experimentally estimating k_0 and finding the value of k_1 using nonlinear optimization to minimize the medium square error (ε) with the following objective function:

$$\min\varepsilon = \sqrt{\frac{1}{n}\sum_i \overline{pNDA_i} - pNDA_i^2} \tag{7}$$

and the following restriction:

$$\overline{pNDA_i} = -\frac{k_0}{k_1} + \left(pNDA_0 + \frac{k_0}{k_1}\right) e^{-k_1 t} \tag{8}$$

where $\overline{pNDA_i}$ is the theoretical amount of pNDA, (μM).

2.6. Bacillus subtilis *spore inactivation tests*

2.6.1. Spore preparation

The strain used in all the experimental assessments was *B. subtilis* (J168). Spores were prepared as described in previous reports [9]. A fresh culture of *B. subtilis* in 2xYT was seeded on 250 mL 2xSG broth. The culture was incubated at 37 °C with mechanical shaking for 5 days and the sample was monitored under a microscope until the cells became spores. At the end of this time period, the culture was centrifuged at 1000 rpm to collect the spores. The supernatant was discarded and the spores were resuspended in cold water, washed, and sonicated until no vegetative cells or debris were observed under the microscope. Finally, the spores were pooled and suspended in 0.01 M phosphate buffer (pH 7.0) to generate a concentrated stock and refrigerated at 4 °C until they were used for the inactivation experiments.

2.6.2. Spore inactivation experiments

Spore preparations used were free (>98%) of growing cells, cell debris, or germinated spores as determined by a phase-contrast microscope examination. All inactivation assessments were performed in sterilized distilled-deionized water using a final spore density of 1.0 at 600 nm (~10^9 spore mL^{-1}). The arrangement for the photoreactor is described in Section 2.2. During the experiments, the spore suspensions were mixed using a conventional stir plate and magnetic bar.

Three different Fe^{2+} concentrations (0.0, 0.10, and 0.25 mM) were tested using the same initial iron/hydrogen peroxide ratio (1/30) reported for the hydroxyl radical production assessments described in Section 2.4. For all experiments, the initial pH of the reaction mixture was adjusted to 3.0 using 0.1 M H_2SO_4, and then the necessary amount of Fe^{2+} was added to the spore suspension to obtain the desired catalyst concentration. The solution was mixed for 1 min in the dark. At this point (t = 0), an initial sample was withdrawn and immediately analyzed for spore viability. Then, hydrogen peroxide was added to the suspension and the reaction mixture was immediately irradiated. The inactivation experiment was considered to have started when irradiation was initiated.

For all of the tests, 100 μL samples were taken every 2.5 min during the first 15 min of reaction time, and then every 15 min during the first hour. Once taken, all the samples were diluted up to 10^7 times using 0.85% sodium chloride solution at pH 7.0. Between every dilution step, the spore suspension was mixed using a vortex to ensure homogeneity and 10 μL of every dilution were inoculated on 2xYT agar. Colonies were visually identified and counted after a 24 h incubation at 37 °C in a microbiological incubator (Isotemp, Fisher Sci).

2.6.3. Influence of radical scavengers

To evaluate the effect of the presence of radical scavengers within the reaction mixture, four different chloride ion concentrations (0.0, 0.3, 0.6, and 1.2 mM) were prepared from Oakton conductivity standard solution of 1413 μS cm^{-1} at 25 °C containing 1 g L^{-1} of total chloride. The radical scavenger was added before the Fenton reagents were added to the mixture and the inactivation experiments were performed as previously described.

3. Results and discussion

3.1. Actinometrical measurements

Fig. 2 shows the values of radiative intensity (I, μEinsteins min^{-1}) entering into the photoreactor at the different distances from the lamp that were tested. As expected, the value of radiative intensity decreases linearly as the distance from the lamp increases. Data from Fig. 2 were fitted ($r^2 = 0.997$) using a linear trend to obtain the following relationship for the decrease in radiative intensity as a function of the distance:

$$I = -1.39D + 39.6 \tag{9}$$

where I is radiative intensity (μEinsteins min^{-1}) and D is the distance from the lamp within the range of x-y cm. As shown in Fig. 2, the experimental radiative-intensity assessments were performed at a distance from the lamp with the highest value of radiative intensity (i.e., at 8 cm from the lamp), which was 28.1 μEinstein min^{-1}.

3.2. Hydroxyl radical production

Fig. 3 shows the change in hydroxyl radical generation against reaction time for the best two Fenton reaction conditions (i.e., $[Fe^{2+}]/[H_2O_2]$ = 0.018/0.55 and 0.036/1.1 mM), which are most representative of the other combinations of reagents tested (data not shown). It is worth noting the increase of the hydroxyl radical production during the first few minutes of the process. In both cases, the trend is that production reaches a plateau during the last

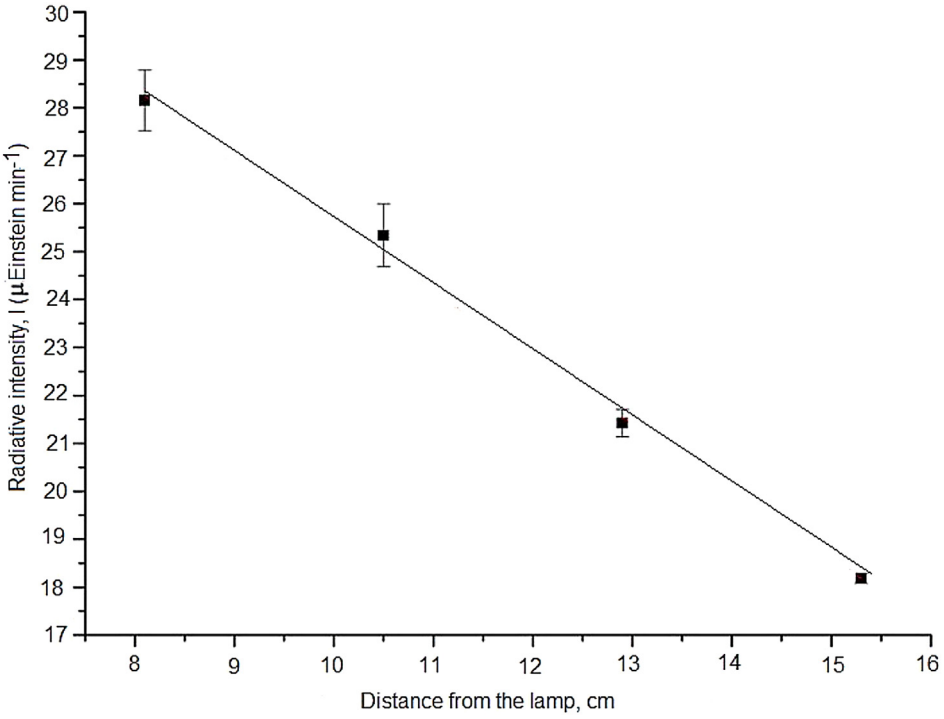

Fig. 2. Radiation intensity values as a function of the distance from the lamps used in the photoreactor.

minutes of the process. Other combinations of Fenton reagents did not show further improvements in the hydroxyl radical production (data not shown). It is worth noting that higher concentrations of Fenton reagents generated the higher hydroxyl radicals. In this case, time may serve as the independent variable because the actinometrical assessments determined radiation flux to be constant.

3.3. Hydroxyl radical production model

The lines included in Fig. 3 represent the results of the kinetic model applied for fitting the experimental data. As shown, the proposed model fits the experimental data fairly well ($r^2 \geq 0.99$). From experimental data of pNDA discoloration without the addition of the Fenton reagents, the photolysis discoloration rate constant was found to be $k_0 = 6.6 \times 10^{-3}\ min^{-1}$. Using this value for the model and the calculations from Eqs. (7) and (8), the values for the hydroxyl radical production ratio were determined to be 1.02×10^{-2} and $3.4 \times 10^{-2}\ min^{-1}$ for high and low Fenton reagent concentrations, respectively, which are shown in Fig. 3. It is notable that hydroxyl production increased three times when the Fenton reagent concentrations were increased two times.

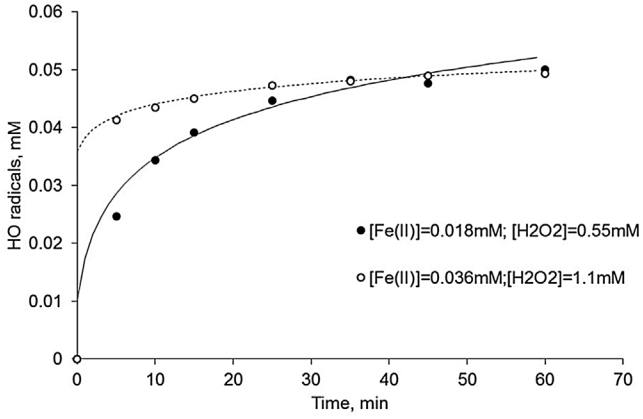

Fig. 3. Hydroxyl radical generation for the photoassisted Fenton process using the best two different reaction conditions tested.

Eq. (6) was used for coupling pNDA photolysis and photocatalytic bleaching. Solution to photolysis-photocatalytic bleaching of pNDA was gotten taking account Eq. (7) and using SOLVER® of Excel®. Using this approximation, the initial hydroxyl radical rate values for the experimental conditions shown in Fig. 3 were estimated as 5 and 8.2 μM min^{-1} for the low and high Fenton reagent concentrations, respectively. If Eqs. (10)–(14) are considered as those involved mainly in the photo-assisted Fenton process [16], from these it is possible to obtain a theoretical photonic efficiency of the process as 2.3 hydroxyl radicals being produced per absorbed photon for the highest reaction conditions.

$$Fe^{2+} + H_2O_2 \rightarrow Fe^{3+} + HO^- + HO^{\bullet} \quad (10)$$

$$Fe^{3+} + H_2O_2 \rightarrow Fe - OOH^{2+} + H^+ \quad (11)$$

$$Fe^{3+} + H_2O \rightarrow [FeOH]^{2+} + H^+ \quad (12)$$

$$Fe - OOH^{2+} + h\nu \rightarrow Fe^{2+} + HO^{\bullet} \quad (13)$$

$$[FeOH]^{2+} \rightarrow [Fe^{2+}] + HO^{\bullet} \quad (14)$$

As proposed in Eqs. (10)–(14), one of the hydroxyl radical produced is probably due to the Fenton reaction (Eq. (10)) occurring between the ferrous iron ion and hydrogen peroxide and the other is produced when the radiation is absorbed in the photo-assisted reduction of the ferric species generated during the Fenton

reaction (Eq. (13)). The amount of hydroxyl radical theoretically produced is slightly higher than two probably due to other side reactions that can occur within the Fenton process that may also produce hydroxyl radicals (e.g., Eq. (14)) as widely reported previously in literature [17].

3.4. Spore inactivation tests

Data from the experimental assessment of the inactivation of *B. subtilis* spores under different reaction conditions are depicted in Fig. 4 as function of photonic flux. As shown, initial pH = 3.0 and UV-A radiation did not affect the survival of spores after being submitted to 2.5 mEinstein of irradiation. These results are not surprising because these types of microorganisms are capable of surviving under very extreme environmental conditions. Past studies have proposed that the effects observed when hydrogen peroxide was added without the addition of iron are because of the photoassisted cleavage of hydrogen peroxide using radiation at a wavelength of 360 nm as proposed by Pignatello et al. [18] from $HO^{\bullet}$ radical production experiments and lately observed for disinfection processes of other microorganisms using Fenton-like processes [6]. This is possible for the results of this study because the radiation used (365 nm) was close to the previously reported wavelength.

As has been previously reported, a significant improvement of the inactivation process was observed when Fenton reagents and UV radiation were used together. Almost 8-log units (99.999999% inactivation) of spore inactivation were achieved after 850 mEinsteins of photonic flux using the mild ($[Fe^{2+}] = 0.1$ mM; $[H_2O_2] = 3.0$ mM, Fe^{2+}/H_2O_2 ratio 30) Fenton reagent concentration. However, it is notable that viable spore count remained unchanged during the first 280 mEinsteins of irradiation. This lag-type phase in which the reaction condition seems have no effect appears not to be related to self-repairing processes that occur within the cells—which has been previously suggested [19] for *E. coli* inactivation using heterogeneous photocatalytic processes—but instead to the effective dose of hydroxyl radicals required to oxidize the main spore structures and achieve inactivation [20]. For *B. subtilis* spores, it has been demonstrated that the main barrier for inactivation is the spore coat [20]. These authors found that no DNA is damaged under hydroxyl radical production, but decoated spores are inactivated within a few minutes of reaction using $CuCl_2$-ascorbic acid in a Fenton-like process. The inactivation trend shown by Shapiro et al. [20] using intact and decoated spores was very similar to the trend in Fig. 4, which shows that chemically decoated spores were inactivated as high as 4-log units (99.99%) within few minutes of reaction and that there was a lag-phase type behavior for intact spores during the initial time of reaction. A similar trend was also found for *cotE* spores (spores that lack proper coat assembly).

When the reaction conditions were changed to use the highest concentration of Fenton reagents (i.e., $[Fe^{2+}] = 0.25$ mM; $[H_2O_2] = 7.5$ mM, Fe/H_2O_2 ratio 30), the spore survival curve decreased almost immediately after the start of the experiment and 9-log units (99.9999999% inactivation) were achieved in approximately 562 mEinstein of irradiation. Previously, we proposed these trends be fitted through delayed Chick-Watson kinetics, in which the independent variable is the accumulated energy that arrives to the system and drives the photocatalytic process demonstrated that the model can accurately describe the observed trend [9]. In this case, another interesting result can be correlated for the actual mechanism that occurs in the inactivation process and the amount of oxidants being generated that are responsible for the process. From the hydroxyl radical production process and the proposed model, it is possible to see a trend for hydroxyl radical production for a specific reaction time. From the model applied to the experimental data of hydroxyl radical production, the amount of HO radicals being generated under the mild experimental conditions tested (i.e., $[Fe^{2+}] = 0.018$ mM and $[H_2O_2] = 0.55$ mM, Fe/H_2O_2 ratio 30) were 0.032 mM after 4.2 mEinsteins of photonic flux. When the reaction conditions were doubled for the highest conditions tested for hydroxyl radical generation (i.e., $[Fe^{2+}] = 0.036$ mM; $[H_2O_2] = 1.1$ mM), the same amount of hydroxyl radicals were achieved after 1.4 mEinsteins of photonic flux. Assuming that the same amount of hydroxyl radicals produced under the conditions tested for photocatalytic inactivation might not be accurate; it could be possible, however, that the ratio of hydroxyl radicals produced might still be the same. Considering this last assumption, the difference in spore-inactivation behavior might be able to be explained as function of the amount of hydroxyl radicals produced for the different reaction conditions tested. The amount of hydroxyl radicals produced under mild conditions (e.g., 5.8×10^{21}) might require the first minutes of the reaction to reach minimum spore-coat damage and increase its sensitivity, whereas this is achieved within just a little over one tenth of the time using the highest reagent concentration and the observed lag phase is avoided, which shows an important decrease in the viable count at the early stages of the process. In agreement with this calculation, the average amount of hydroxyl radicals being able to interact with every spore can be estimated

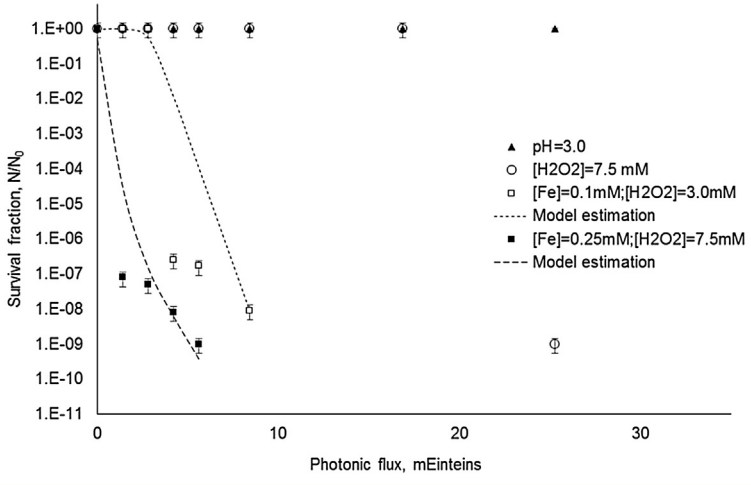

Fig. 4. Inactivation of *B. subtilis* spores for different reaction conditions of the photoassisted Fenton reaction.

-considering the initial count of spores (e.g., 10^9) and the amount of hydroxyl radical produced during the starting 4.2 mEinsteins of photonic flux in agreement with the proposed kinetic model (e.g., 5.8×10^{21})- as 5.8×10^{12}. Palop et al. [21] and Palop et al. (1998) suggested that hydroperoxides inactivate spores by damaging spore core enzymes. However, this mechanism is not clear and there is some controversy about whether or not this is the cause of inactivation. Based on the experimental results reported by Shapiro et al. [20], we believe that core enzyme damage may not need to be considered for hydroxyl radical producing processes such as the Fenton and Fenton-like reactions used in this study but the damage caused by the hydroxyl radicals to the external spore coat.

In order to show the correlation between the hydroxyl radical production estimated from the proposed model and the spore inactivation, the experimental data for the photo-assisted Fenton reaction showed in Fig. 4 were fitted using a modified Fermi model as proposed in Eq. (14):

$$S\left(HO^{\bullet}\right) = \left[\frac{1}{1 + e^{\left(\frac{HO^{\bullet} - HO_c^{\bullet}}{k_{in}}\right)}}\right] \tag{14}$$

where $S\left(HO^{\bullet}\right)$ is the fraction of surviving organisms after the application of a given amount of hydroxyl radicals generated using the photo-assisted Fenton reaction, $HO^{\bullet}$ is the amount of hydroxyl radical produced for an specific value of photonic flux, $HO_c^{\bullet}$ is the critical level of hydroxyl radicals at which the surviving fraction is equal to a half of the initial count, and k_{in} is a constant that indicates the steepness of the survival curve around $HO_c^{\bullet}$. In this modified Fermi model for microorganism inactivation the hydroxyl radical production estimated using the model described in Section 3.3 was used instead of the accumulated energy or temperature as the main driving force for the inactivation process as reported in the past [8,22]. The results of using the Fermi model described earlier for the experimental data of inactivation of *B. subtilis* spores are also shown in Fig. 4 as dotted lines. As shown, the Fermi model proposed fit reasonably the experimental data for the two reaction conditions showed and reflex the effect of the increase on the Fenton reagents on the hydroxyl radical production and, consequently, spore inactivation. It is worth to mention that, despite the overall shape of the dose-response curves for the spore inactivation is described by the Fermi model proposed, it failed in predicting the results at the initial stages of the inactivation process. This is probably due to the process used for estimating the $HO_c^{\bullet}$ value because as the process was able to inactivate over 7-log units within the first 0.5 mEinsteins of irradiation, the critical level of hydroxyl radical at which the surviving fraction is equal to a half of the initial count was estimated by simple interpolation.

3.5. Influence of radical scavengers

The spore inactivation process and the presence of radical scavengers were tested to provide additional information to support the proposed mechanism. Chloride ions have been widely reported to be hydroxyl radical scavengers and capable to react with the Fenton reagents, which is shown in Eqs. (15)–(17) [23,17] as follows:

$$HO^{\bullet} + Cl^{-} \rightarrow [ClOH]^{\bullet -} \tag{15}$$

$$\left[Fe^{2+}\right] + Cl^{-} \leftrightarrow FeCl^{-} \tag{16}$$

$$\left[Fe^{3+}\right] + Cl^{-} \leftrightarrow FeCl^{2+} \tag{17}$$

Fig. 5 shows the effect of addition of hydroxyl radical scavengers within the reaction mixture. The results show that even adding the lowest concentration of chloride ions has a significant effect on the inactivation process. The lag phase that was observed for low concentrations of Fenton reagents appeared again in the inactivation curve during the first 3 mEinstein of photonic flux when 0.3 mM of chloride ions were added. After that initial lag-phase, a significant decrease in the viable spore count (almost an 8-log decrease) was observed over the following 2 mEinstein. The same trend was observed when further increases in the chloride ion concentration (i.e., 0.6 and 1.2 mM) were tested. This results can also be explained using the hydroxyl radical model described earlier, in agreement with the model 0.48 mM of hydroxyl radicals will be generated under the conditions tested after the initial

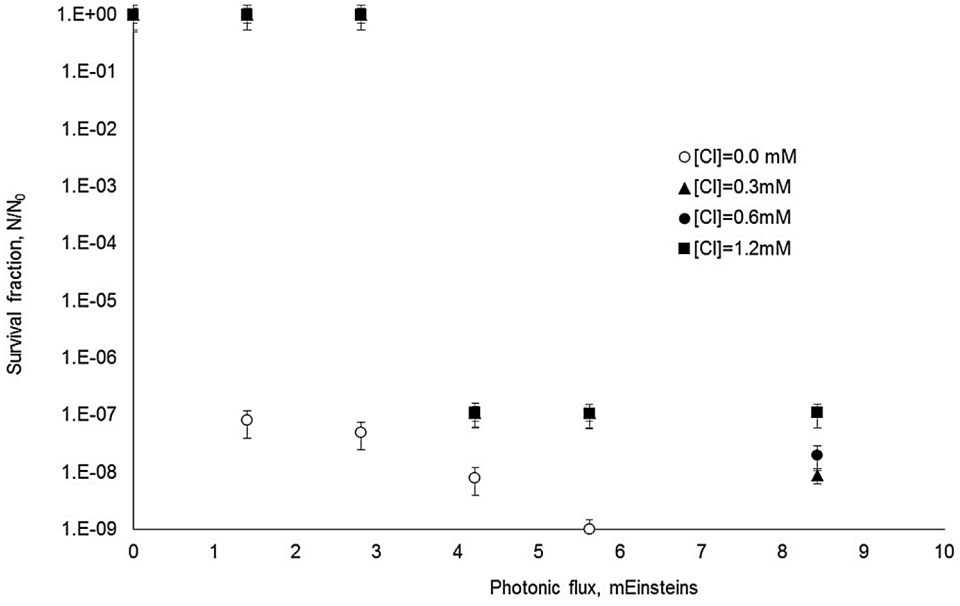

Fig. 5. Effect of different concentrations of radical scavengers (chloride ion) on the inactivation of *B. subtilis* spores.

2.8 mEinstein of phonic flux. From Eq. (15) the stoichiometry of the reaction among hydroxyl radicals and chloride ions is expected to be 1:1 so the amount of hydroxyl radical produced will over number the amount of chloride ions being capable to start with the inactivation process but only after few minutes of reaction generating the lag-phase to appear once again in the experimental runs. The continuous production of hydroxyl radical as the irradiation continue may give rise to further inactivation for the low chlorine ions concentration except for the higher value where no further changes were observed probably because higher amount of irradiation or reagents concentration may be needed to match the excess of chlorine ions added.

The effect of chloride ions observed agrees with previously reported results for the use of hydroxyl radical generation to discolor dyes [23]. The authors observed slight decreases in discoloration when a chloride ion concentration below 100 mM was added to the reaction mixture and significant decreases in discoloration when chloride ion concentrations were higher than 100 mM, but that discoloration remained constant when the chloride concentration reached 1250 mM.

This study showed that the system was more sensitive to chloride ion concentration than what was observed in previous studies because even the lowest concentration caused a significant decrease in the reaction rate. These results might be because chloride ions react with hydroxyl radicals to generate hypochlorite radical anions ($HOCl^{\bullet -}$) that further react with hydronium ions at low pH values (i.e., lower than 7.2) to generate chlorine radicals $Cl^{\bullet}$ and other side reactions that form several other radical species with lower oxidative capabilities than hydroxyl radicals [24,25]. These species might be capable of inactivating spores, but this process is expected to be significantly less effective than the hydroxyl radical process.

The results from this study disagree with the results reported by Shapiro et al. [20], who found that adding chloride ions improved the reaction rate and generated a significant increase in spore inactivation. However, this discrepancy might be because of differences in the hydroxyl radical generation process used. Shapiro et al. [20] used the copper(II)-ascorbic acid system for OH radical production, whereas we used the iron(II) hydrogen peroxide couple. The former process is widely known to be rate dependent on the chloride ion concentration [26] and has shown that medium to high chloride ion concentrations (i.e., 1.6–500 mM of Cl^-) produce significant increases in the oxidation process [27]. The chloride ion concentrations tested by Shapiro et al. [20] fall within this concentration range, so the observed increase in the inactivation rate is expected. Additionally, high amounts of chloride ions might create hypertonic conditions that affect the germination process. This study used very low chloride concentrations to avoid hypertonic conditions, which suggests that chloride ions may only have a scavenging effect on the hydroxyl radicals that would consequently affect the inactivation process under the tested conditions.

4. Conclusions

The inactivation of *Bacillus subtilis* spores in water was successfully achieved using a photoassisted Fenton reaction under mild reaction conditions. Up to 8-log units of spore inactivation was achieved under the best reaction conditions. Lower reagent concentrations or using hydrogen peroxide alone (without iron addition) under radiation produced lower spore inactivation and a lag-type phase in which no inactivation seemed to occur. The inactivation mechanism was indirectly related to the radiation dose and hydroxyl radical generation using the photocatalytic process. The amount of OH radicals produced was related to the reaction conditions based on the experiments carried out using a widely reported hydroxyl radical scavenger. Assuming that the amount of hydroxyl radicals produced under the reaction conditions used in the photocatalytic discoloration process remained within the same ratio when spore inactivation was tested, the effect of process conditions on the actual decrease in viable spore counts was a function of the amount of OH radicals being generated. Similarly, the observed lag-type phase was related to reaction conditions in which the required dose of oxidants had not been achieved. Once the required amount of OH radicals was produced and acted against the spores, there was a decrease in active counts that moved quickly until significant inactivation values were reached. The resulting model agreed with previous study results that tested other hydroxyl-radical-producing processes. The proposed mechanism for spore inactivation, including spore coat damage by the action of the hydroxyl radicals instead of the effect of these species on core spore enzymes, was also tested by adding chloride ions as the radical scavenging species. Adding chloride ions, even at a low concentration, significantly decreased the efficiency of the inactivation process compared with tests in which no scavenger was added. Also, a lag-type phase was observed when scavengers were added even under the best reaction conditions. This suggests that chloride ions might compete for the hydroxyl radicals generated under the reaction conditions tested and produce the observed delay in the inactivation process. More research is required to describe the actual inactivation mechanism that occurs during the process, but this work highlights some findings that could lead to a better understanding of the process and demonstrates the value of further research on the inactivation mechanism.

Acknowledgments

This material is based upon work supported in part by the National Science Foundation (grant IIA-1301726) and CONACyT Mexico (grant CB-2011-01-168285). L.C. Huesca thanks CONACyT and UDLAP for providing her with a scholarship to pursue her doctoral studies. The authors are also grateful to Ms. Nicole Damon (DRI) for her editorial review.

References

[1] E.R. Bandala, E. Bustos, Photocatalytic materials in water disinfection, in: A. Hernandez-Ramirez, I. Medina-Ramírez (Eds.), Photocatalytic Semiconductors: Synthesis, Characterization and Environmental Applications, Springer, London, UK, 2015, pp. 255–278.
[2] B.A. Smith, T. Ruthmann, E. Sparling, H. Auld, N. Comer, I. Young, A.M. 14 Lammerding, A. Fasil, A risk modeling framework to evaluate the 15 impacts of climate change and adaptation on food and water safety, Food Res. Int. 68 (2014) 78–85.
[3] IPCC, Climate Change 2013: The Physical Science Basis. Contribution of Working Group I to the Fifth Assessment Report of the Intergovernmental Panel on Climate Change, Cambridge University Press, Cambridge, United Kingdom and New York, NY, USA, 2013.
[4] M.C. Tirado, R. Clarke, L.A. Jaykus, A. McQuatters-Gollop, J.M. Frank, Climate change and food safety: a review, Food Res. Int. 43 (7) (2010) 1745–1765.
[5] J. Semenza, S. Herbst, A. Rechenburg, J.E. Suk, C. Höser, C. Schreiber, Climate change impact assessment of food- and waterborne diseases, Crit. Rev. Environ. Sci. Technol. 42 (8) (2012) 857–890.
[6] E.R. Bandala, L. Gonzalez, F. De la Hoz, M. Pelaez, D.D. Dionysiou, P.S.M. Dunlop, J.A. Byrne, J.L. Sanchez, Application of azo dyes as dosimetric indicators for enhanced photocatalytic solar disinfection (ENPOSODIS), J. Photochem. Photobiol. A Chem. 218 (2011) 185–191.
[7] E.R. Bandala, J.H. Castillo-Ledezma, L. González, J.L. Sánchez-Salas, Solar driven advanced oxidation processes for inactivation of pathogenic microorganisms in water, Recent Res. Dev. Photochem. Photobiol. 8 (2011) 1–16.
[8] V. Aurioles-Lopez, M.I. Polo-Lopez, P. Fernandez-Ibanez, A. Lopez-Malo, E.R. Bandala, Effect of iron salt counter ion in dose-response curves for inactivation of Fusarium solani in water through solar driven Fenton-like processes, Phys. Chem. Earth 91 (2015) 46–52.
[9] E.R. Bandala, R. Perez, A.E. Velez-Lee, J.L. Sanchez-Salas, M.A. Quiroz, M.A. Mendez-Rojas, *Bacillus subtilis* spore inactivation in water using Photo assisted Fenton reactions, Sustain. Environ. Res. 21 (2011) 285–290.

[10] E.R. Bandala, L. Gonzalez, J.L. Sanchez-Salas, J.H. Castillo-Ledezma, Inactivation of *Ascaris* eggs in water using sequential solar driven photo-Fenton and free chlorine, J. Water Health 10 (2012) 20–30.
[11] E.R. Bandala, B.W. Raichle, Solar driven advanced oxidation processes for water decontamination and disinfection, in: N. Enteria, A. Akbarsadeh (Eds.), Solar Energy Sciences and Engineering Applications, CRC Press, London, UK, 2013, pp. 395–412.
[12] R. Guisar, M.I. Herrera, E.R. Bandala, J.L. García, B. Corona, Inactivation of waterborne pathogens using solar photocatalysis, J. Adv. Oxid. Technol. 10 (2007) 1–4.
[13] M. Montalti, A. Credi, L. Prodi, M. Gandolfi, Handbook of Photochemistry, CRC Press, U.S, 2006.
[14] H.J. Kuhn, E. Braslavky, R. Schmidt, Chemical actinometry: IUPAC technical report, Pure Appl. Chem. 76 (12) (2004) 2105–2146.
[15] S.L. Murov, I. Carmichael, G.L. Hug, Handbook of Photochemistry, Marcel Dekker Inc., USA, 1993.
[16] J.M. Chacon, M.T. Leal, M. Sanchez, E.R. Bandala, Solar photocatalytic degradation of azo-dyes by photo-Fenton process, Dyes Pigm. 69 (2006) 144–150.
[17] S.L. Orozco, E.R. Bandala, C.A. Arancibia, B. Serrano, R. Suarez-Parra, I. Hernandez-Perez, Effect of iron salt on the color removal of water containing the azo-dye reactive blue 69 using photo-assisted Fe(II)/H_2O_2 and Fe(III)/H_2O_2 systems, J. Photochem. Photobiol. A Chem. 198 (2008) 144–149.
[18] J. Pignatello, D. Liu, P. Huston, Evidence for an additional oxidant in the photoassisted Fenton reaction, Environ. Sci. Technol. 33 (1999) 1832–1839.
[19] J.H. Castillo-Ledezma, J.L. Sanchez-Salas, A. Lopez-Malo, E.R. Bandala, Effect of pH solar irradiation, and semiconductor concentration on the photocatalytic disinfection of Escherichia coli in water using nitrogen-doped TiO_2, Eur. Food Res. Technol. 233 (2011) 825–834.
[20] M.P. Shapiro, B. Setlow, P. Setlow, Killing of *Bacillus subtilis* spores by a modified Fenton reagent containing $CuCl_2$ and ascorbic acid, Appl. Environ. Microbiol. 70 (4) (2004) 2535–2539.
[21] A. Palop, G.C. Rutherford, R.E. Marquis, Hydroperoxide inactivation of enzymes within spores of Bacillus megaterium ATCC 19213, FEMS Microbiol. Lett. 142 (1996) 283–287.
[22] A. Lopez-Malo, S.M. Alzamora, E. Palou, Aspergillus flavus dose response curves to selected natural and synthetic antimicrobials, Int. J. Food Microbiol. 73 (2) (2002) 213–218.
[23] I. Gultekin, N.H. Ince, Degradation of reactive azo dyes by UV/H_2O_2: impact of radical scavengers, J. Environ. Sci. Health A39 (4) (2004) 1069–1081.
[24] C.H. Liao, S.F. Kang, F.A. Wu, Hydroxyl radical scavenging role of chloride and bicarbonate ions in the H_2O_2/UV process, Chemosphere 44 (2001) 1193–1200.
[25] J. Kiwi, A. Lopez, V. Nadtochenko, Mechanism and kinetics of the OH radical intervention during Fenton oxidation in the presence of a significant amount of radical scavenger (Cl), Environ. Sci. Technol. 34 (2000) 2162–2168.
[26] J. Xu, R.B. Jordan, Kinetics and mechanism of the reaction of aqueous copper (II) with ascorbic acid, Inorg. Chem. 29 (16) (1990) 2933–2936.
[27] M.J. Sisley, R.B. Jordan, Kinetic study of the oxidation of ascorbic acid by aqueous copper(II) catalyzed by chloride ion, J. Chem. Soc. Dalton Trans. (1997) 3883–3888.